國立臺灣師範大學生命科學系碩士論文

斑馬魚仔魚體表排氨功能與機制之研究

Ammonia secretion by the skin of zebrafish (*Danio rerio*) larvae

研 究 生：施廷翰

Tin-Han Shih

指導教授：林豐益 博士

Li-Yih Lin

中華民國九十七年六月

誌謝

最大的感謝要獻給**林豐益**老師。由於老師的悉心栽培，我的研究之路才得以獲得啟蒙。感謝老師給予的鼓勵與教導，使我的研究能夠修成正果。感謝老師買便當之際仍三不五時會請客一頓，減輕了我生活上的不少煩惱。也感謝**君琳**學姐以及**文庭**弟弟，能夠分散老師的注意力，讓老師在研究之餘能夠調適身心。

感謝身為楷模的**黃鵬鵬**老師，您的想法總是這麼地有見地。感謝**張清風**老師與**林惠真**老師，細心地幫我修正論文中的種種缺失，老師們的建議，開拓了我研究方向的視野。也感謝**黃基礎**老師與**呂國棟**老師，在我修課過程中帶給我更寬廣的學識經歷。

感謝**君琳**學姐像大姐頭般的照顧，還有**家俊**學長的神秘技術指導，使我的研究得以有所進展。感謝實驗室**鶴文**學長的貼心問暖，還有**淑貞**學姐所提供的生活非必需品，讓我在實驗之餘心靈能夠有所洗滌。感謝許多師大的學長同學，吳姊**世郁**與賴姊**亭諭**，真是不可多得的好友。吳哥**民聰**在動生實驗的教導讓我受益良多，作豪**老唐**的閒暇逸樂則是有助吾人凡身的昇華。**寬哥**、**曜如**，**許大博**、希望接下來的日子可以跟你們這些哥兒們一起打拼。感謝**仁華**、**琬婷**、**惠如**、**欣燁**，身為飯友的你們真的很稱職，謝謝你們在生活上的許多幫助。感謝師大第一勇士**孟緯**，這世界似乎阻止不了你的豪氣。也感謝附中之光**怡帆**學長，你人很好，真的。感謝**貫捷**還有**正國**的情義相挺，也感謝中研院一票子的老大哥老大姊以及一起努力的兩位同學**咸媽**及**純爸**。特別感謝**峻爺**及其斑馬魚子弟兵，還有**王哥**的諸多幫忙。

感謝**施爸爸**及**施媽媽**的支持，有了你們在背後當我的支柱，我才能繼續往前邁進。感謝**台南王家二姑娘**，在我徬徨無助的時候總是陪伴在我身邊，你的存在就是我的動力來源。

施廷翰 民國 97 年 6 月

Table of Contents

Abstract

The most effective route for fishes to deal with toxic nitrogenous wastes is to excrete NH_3/NH_4^+ into water directly. Over 80% of total ammonia in fish body is excreted into water via the gill epithelium. However, the mechanism for branchial ammonia transport of freshwater fish is not well understood. Using zebrafish larvae as a model, the present study investigated the mechanism of ammonia secretion by the skin of the larvae. Scanning ion-selective electrode technique (SIET) was applied to detect the NH_4^+ and H^+ fluxes at specific cells of larval skin. NH_4^+ extrusion was relatively high in H^+ pump-rich cells (HRCs), which were identified as the H^+-secreting ionocyte in zebrafish. Minor NH_4^+ extrusion was also detected in keratinocytes and other types of ionocytes in larval skin. NH_4^+ secretion from the skin was tightly linked to acid secretion. Increases in the external pH and buffer concentration (5 mM MOPS, 3-morpholinopropane sulfonic acid) diminished H^+ and NH_4^+ gradients at the larval surface. Moreover, coupled decreases in NH_4^+ and H^+ extrusion were found in larvae treated with an H^+-pump inhibitor (bafilomycin A1) or H^+-pump gene (*atp6v1a*) knockdown. Knockdown of Rhcg1 (*drrhcg1*) also decreased NH_4^+ secretion at larval skin and HRCs. This study demonstrates ammonia secretion in epithelial cells of larval skin through an acid-trapping mechanism, and provides direct evidence for the involvement of the H^+ pump and an Rh glycoprotein (Rhcg1) in ammonia secretion.

摘要

淡水魚類移除體內含氮廢物最佳的方式，是直接將廢物以氨(ammonia，即 NH_3 與 NH_4^+)的形式排放到水體。具研究顯示，80%以上的氨會經由鰓排出。然而目前針對魚類鰓表皮細胞所作的研究仍未足以提供直接的證據說明排氨的運行方式。本實驗選用斑馬魚仔魚為模式動物，透過其體表的離子調節功能探討淡水魚類的排氨機制。

在本實驗中，利用掃描式離子選擇性電極技術（Scanning Ion-selective Electrode Technique, SIET）對仔魚體表離子作檢測。實驗發現在富含氫幫浦細胞(HRC）上的排氨的程度高於周遭的平舖細胞（PVC）與其它類型的離子細胞(Ionocyte)。以往的研究推論氫離子（H^+）與排氨之間有密切的關係。在本實驗中，針對氫幫浦而使用的抑制劑 bafilomycin A1 與 gene knockdown 技術，會同時造成魚類 H^+ 與 NH_4^+ 的梯度顯著降低。當給予水體高量緩衝溶液（5 mM 3-morpholinopropane sulfonic acid, MOPS）時，也發現 H^+ 與 NH_4^+ 的排出量顯著下降。本實驗亦以 SIET 分析 Rhcg1 的功能，發現 *rhcg1* knockdown 的仔魚其體表以及細胞排氨量明顯降低。綜合以上結果，本實驗證實仔魚體表細胞透過酸捕捉機制進行排氨功能，也為氫幫浦及 Rhcg1 提供參與排氨機制的直接證據。

Introduction

Ammonia production in fish

Ammonia (including NH_3 and NH_4^+) is a toxicant that being poisonous to animals. Under normal situation, over a half of dietary nitrogen-content is converted into amino acids then used by the anabolism of structural growth. Ammonia occurs as the product of transamination of amino acids followed by the deamination of glutamate (Walsh, 1998).

Toxicity of ammonia

Ammonia can exist as ammonium (NH_4^+) and a water-soluble gas state NH_3. The equilibrium of NH_3 and its protonated form is simplified as follow

$$NH_3 + H^+ \Leftrightarrow NH_4^+$$

Total ammonia concentrations (T_{Amm}, NH_3 and NH_4^+) in fish body are ranged from 0.05 mM to 1 mM (Wood, 1993), depending on the fish species. Being the most elementary form of nitrogen contents, ammonia will be useful in the reconstructing of amino acids. However, it is toxic to accumulate ammonia in the body.

With a hydrated radium and charge density similar to K^+, NH_4^+ is believed to be capable of substituting K^+ ion in ion transporters and protein channels like $Na^+/K^+/2Cl^-$ cotransporter and K^+ channel and somehow depolarizing cell membrane (Allert et al., 1998). Substitution of

K^+ channels in central nervous system may disrupt the electrochemical gradient (Cooper and Plum, 1987), leading an over activation of downstream receptors like glutamate NMDA receptors. Swelling of neurons by astrocytes is happened when glutamine is accumulated through the excessive activation of NMDA receptors. To prevent acute brain damage, ammonia needs to be excreted into environment.

Ammonia excretion in fish gills

Different from terrestrial animals which need extra energy consumption to excrete nitrogenous wastes as urea for water conservation, the most convenient excretory route for fishes is to excrete ammonia into water directly. In ammonotelic fishes (which excrete most nitrogenous wastes as ammonia), organs such as kidney, skin and even intestine are involved in ammonia excretion. The majority of ammonia, however, has been suggested to excrete from the gills. According to the highest ventilation rate, gill is the most proper site for substrate exchange, being responsible for over 80% ammonia excretion in fish (Wood, 1993). Plasma T_{Amm} was sent to gill in an elevated concentration relative to water environment, contributing a down-favorable gradient for ammonia excretion.

Ammonia excretion in freshwater fishes

There are two major excretory mechanisms by which ammonia can pass from plasma through the gill of freshwater fishes into environment (Wilkie, 2002; Evans et al., 2005). These two distinct routes are: (1) NH_3

passive diffusion and (2) NH_4^+ active transport.

(1). NH_3 diffusion

Considering the physicochemical properties of NH_3, it is appropriate to excrete ammonia through NH_3 diffusion (Evans and Cameron, 1986). Evidences supporting passive NH_3 diffusion mostly based on the observations of blood-to-water gradient. As calculated by Cameron and Heisler (1983), NH_3 diffusion of rainbow trout under resting condition is adequate for ammonia excretion. In an isolated-perfused head experiment of rainbow trout (Avella and Bornancin, 1989), diffusive movement of NH_3 appears to account for the ammonia efflux according to the estimation of diffusion and permeability coefficients. In addition, ammonia flow is inhibited when the gradient is reduced by high ambient ammonia (Avella and Bornancin, 1989; Wilson et al., 1994).

H^+ gradient facilitates NH_3 diffusion

Wright et al. (1989) suggested that maintenance of the transbranchial ammonia gradient relies on acidification of unstirred layers of the apical surface of the branchial epithelium. As it is acidified, this layer creates a microenvironment for a favorable transbranchial NH_3 gradient that facilitates ammonia excretion. This is especially advantageous during exposure to high ammonia (HA), which reverses the normally positive ammonia gradient. Abolishing this layer with HEPES buffer during HA reduced the net efflux of total ammonia (Wilson et al., 1994). Although the proton plays an important role in ammonia excretion, there still lack

of functional evidences to support the idea of acid trapping model. It was suggested that H^+ arising from CO_2 hydration is the main source of boundary layer acidification (Wright et al., 1989). However, the proposed mechanism has been debated.

Another mechanism was explained by the discovery of gill V-type H^+-ATPase (Wilkie, 2002). Recent evidence has shown that the branchial surface might also be acidified by H^+ extruded from an apical vacuolar H^+-ATPase. Recent data using pharmacological, physiological, immunocytochemical, and molecular approaches have demonstrated the role of V-type H^+-ATPase in the apical Na^+ uptake mechanism of freshwater teleosts (Claiborne et al., 2002; Hwang and Lee, 2007). Nawata et al., (2007) reported that the gill H^+-pump mRNA expression was elevated in high ammonia exposed rainbow trout. However, direct evidence for this assumption is still lacking. The present study attempted to demonstrate this mechanism.

(2) NH_4^+ active transport

In the past few decades, researchers had discovered that J_{Amm} were decreased upon the usage of Na^+/H^+ exchanger (NHE) inhibitor (amiloride) and Na^+/K^+-ATPase (NKA) inhibitor (ouabain), indicating an active transport of NH_4^+ by these proteins (Wilkie, 2002). In this model, NH_4^+ is carried from plasma to gill via basolateral NKA, by which NH_4^+ substitute K^+, and transport into water through apical membrane NHE by means of actively NH_4^+/Na^+ exchange. Studies on mudskipper which live in NH_3 diffusion unfavorable water found that gill NKA activity were

increased after the exposure of high ammonia, accompanied the inhibition of J_{amm} by ouabain and amiloride (Randall et al., 1999; Wilson et al., 2000b). Another evidence for active NH_4^+ transport is relied on the investigation of Osorezan dace (*Tribolodon hakonensis*) living in extreme acid lake (Hirata et al., 2003). In acid water, Osorezan dace displayed increasing NHE and glutamine dehydrogenase (GDH) expression. It was consequently hypothesized that active branchial ammonia excretion in dace gills take place by the secretion of over produced NH_4^+ via NHE. Although, the NHE has been identified in gills of several freshwater species including rainbow trout (*Oncorhynchus mykiss*) (Wilson et al., 2000a), tilapia (*Oreochromis mossambicus*) (Wilson et al., 2000a), Osorezan dace (*Tribolodon hakonensis*) (Hirata et al., 2003), and zebrafish (*Danio rerio*) (Yan et al., 2007), the contribution of the apical NHE to ammonia transport has been debated (Wilson et al., 1994; Nawata et al., 2007).

Rhesus glycoproteins in ammonia transport

A new mechanism for demonstrating fish ammonia excretion has been discussed recently is that Rhesus glycoproteins (Rh proteins), although the molecular mechanism is still unclear. Rh protein which is also distributed on the membrane of red blood cells (Rh blood type) has been found to be involved in mammalian ammonia transport (Winkler, 2006; Weiner and Hamm, 2007). Based on the structure analysis of Amt (a homologous protein of Rh glycoproteins) by Khademi et al. (2004), the most accepted route is that Rh glycoproteins can conduct ammonia as the

form of NH_3. In mammal, 3 isoforms of Rh glycoproteins were identified as the erythroid RhAG and the non-erythroid RhBG and RhCG (Huang and Liu, 2001; Weiner, 2006).

Rh glycoproteins in fishes

Several Rh-related proteins have been reported in several teleosts, including pufferfish (*Takifugu rubripes*, Nakada et al., 2007b), killifish (*Kryptolebias marmoratus*; Hung et al., 2007), rainbow trout (Nawata et al., 2007) and zebrafish (Nakada et al., 2007a). Despite the whole body expression of Rhbg, the two Rhcg isoforms, Rhcg1 and Rhcg2, are located in the gills of rainbow trout (Nawata et al., 2007). During high ammonia (HA) exposure, expression of gill Rhcg2 mRNA increased to a significant level in pavement cells, but not in MRCs. In another study (Nakada et al., 2007a), zebrafish gill Rhcg1 is localized to the apical region of H^+ pump-rich cell (HRC), which is an ionocyte characterized in secreting H^+ (Lin et al., 2006). Although the Rh proteins have been found in fishes, however, direct evidence has never been reported.

Zebrafish larvae as a model

It is advantageous for using zebrafish as a model to study ion regulation. Skills about gene knockdown by morpholino oligonucleotides and gene overexpress by mRNA injection in zebrafish have become polular in the near years (Hwang and Lee, 2007). Two subtypes of ionocytes, HRC (H^+ pump-rich cells) and NaRC (Na^+ pump-rich cells),

had been identified in zebrafish larva by molecular and electrophysiological approaches (Lin et al., 2006). Knockdown of H^+-ATPase translation with specific morpholino oligonucleotides (MOs) (Horng et al., 2007) and bafilomycin inhibition (Lin et al., 2006) demonstrated that H^+-ATPase contributes to acid secretion in the skin of zebrafish larvae. Basing on those achievements, the present study attempted to investigate the mechanism of ammonia secretion by using electrophysiological technique (SIET) and the zebrafish model.

Purpose

Ammonia is suggested to be excreted via gill epithelial cells, which contains two major cell types, pavement cells (PVCs) and mitochondria-rich cells (MRCs). However, direct evidence has never been reported to compare the ammonia transport in these two cell types. In addition, as noted in above introduction, acid-trapping mechanism is a dominant model for ammonia excretion. However, direct evidence linking H^+-ATPase, Rh protein and ammonia transport is still lacking. In this study, we attempted to use a non-invasive technique (Sacnning ion-selective electrode technique, SIET) to locate and quantify ammonium flux in zebrafish larvae and test a hypothesis that H^+-ATPase and Rh protein in skin HRCs are involved in the mechanism of ammonia excretion.

Specific aims:

(1). To measure NH_4^+ secretion in the skin of zebrafish larvae and compare the function of specific skin cell type.

(2). To test the acid-trapping mechanism in zebrafish larvae

(3). Using inhibitors and gene knockdown technique to examine the contribution of H^+-ATPase, NHE, and Rhcg1 to NH_4^+ secretion.

(4). Analyzing the mRNA expression of H-ATPase, NHE, Rhcg1, Rhcg2 in zebrafish gill epithelium.

Materials and Methods

Zrbrafish

Mature wild type AB strain of zebrafish (*Denio rerio*) was obtained from stocks of Institude of Cellular and Organismic Biology, Academia Sinica, and maintained as described in “ The Zebrafish Book ”. Fish were reared in aquatic tank at 28°C water temperature under illumination cycle as 14 hr brightness / 10 hr darkness. Eggs were collected from mating pairs about 1 hr after being laid.

Artificial water and high ammonia treatment

Fertilized eggs were incubated in normal water (NW, pH 7.0) containing (in mM) 0.5 NaCl, 0.2 $MgSO_4$, 0.2 $CaSO_4$, 0.005 KH_2PO_4 and 0.08 K_2HPO_4. High ammonia (HA) exposed larvae were acclimated to NW with NH_4Cl. Daily exchange of medium is necessary to keep pH and ion concentrations. Adult zebrafish for qRT-PCR analysis (see below) were acclimated to NW or 5 mM HA water for 5 days without feeding. HA water was renewed every day.

Scanning Ion-selective Electrode Technique (SIET)

To measure the specific ion activities at the surface of zebrafish larvae, ion-selective microelectrodes for NH_4^+ and H^+ were constructed. Glass capillary tubes (World Precision Instruments, Sarasota, FL; no. TW 150-4 with 1.12- and 1.5-mm inner and outer diameters, respectively)

were pulled by Sutter P-97 Flaming Brown pipette puller (Sutter Instruments, San Rafeal, CA) into microelectrodes with tip diameters of 3-4 μm. Glass microelectrodes then baked in covered dishes at 120 °C overnight in order to extrude water vapor, and silanized with dimethyl chlorosilane (Fluka, Buchs, Switzerland) for 30 minutes. The covers were removed before further baking at 120°C for at least 1 hour.

Microelectrodes were constructed as following steps. Capillaries were backfilled with 1 cm column of 100 mM NH_4Cl and 40 mM KH_2PO_4 / 15 mM K_2HPO_4 for NH_4^+ and H^+ electrode, respectively. Then the electrodes were frontloaded with a 20-30 μm column of liquid ion exchanger cocktail (LIX cocktail; Ammonium ionophore 1 and Hydrogen ionophore I-cocktail B; Fluka). Selective microelectrodes were connected to an operational amplifier (IP Amp, Ion Polarographic Amplifier; Applicabe, Electronics, East Falmouth, MA) via an Ag/AgCl wire electrode holder and the positioning of electrode was achieved with a stepper-motor-driven three-dimensional positioner (Applicabel Electronics. East Falmouth, MA). The microelectrode system was attached to an Olympus upright microscope (model BX-50WI) and the system circuit was completed by placing a salt bridge made form 3 M KCl in 3% agarose and connected to a Ag/AgCl wire.

Data acquisition, preliminary processing and control of 3-D electrode positioner were performed with ASET software (Sience Wares, East Falmouth, MA). The Nernstian properties of each microelectrode were measured by placing the electrode in a series of standard NH_4Cl and pH solutions (NH_4Cl 0.1, 1, 10 mM; pH 6, 7, 8). By plotting the voltage output of probe against the log NH_4^+ and H^+ concentration, a linear

regression yielded a Nernstian slope of 57.85 ± 0.6 (NH_4^+ probe, n = 10) and 57.5 ± 2.5 (H^+ probe, n = 10) were yield.

Measurement of surface NH_4^+ and H^+ gradient

The measurement was performed at room temperature (26-28°C) in a small plastic recording chamber filled with 1 ml "recording medium" which contained 300 μM MOPS buffer and 0.1 mg/L ethyl 3-aminobenzoate (tricaine) at pH 7.0. The anesthetized embryo was positioned in the center of the chamber with its lateral side contacting the base of the chamber. To record the larva surface ion gradient, the ion-selective probe was moved to target positions. Voltage output signals in millivolts were recorded and analysis. In this study, $\Delta[NH_4^+]$ and $\Delta[H^+]$ were respectively used to represent the measured NH_4^+ and H^+ gradients between the point of interest (skin surface) and background. Value for calculation of ion concentration is converted from ion activities (in mV) after three-point calibration.

Calculation of NH_4^+ flux in ionocytes and keratinocytes

An anesthetized larva was laid laterally in the chamber for the following measurement. Under the DIC microscope, the apical membrane of ionocytes could be identified easily in the skin covering the entire larva. Due to the numerous granules, apical openings of ionocytes on yolk sac surface are barely identified. Therefore, most ionocytes measured in this study were distributed on the skin covering the lateral side of the body trunk, which also served as a suitable flat plane for probing. To detect

local NH_4^+ flux generated by specific cells, the probe was seted to 2-3 μm above the surface spot of interest cell. Cell flux measurement was completed by vibrating microelectrode in an orthogonal (z) direction with a distance of 10 μm. The “wait” and “sample” periods were 0.3 and 0.7 s, respectively. A ”line scan” was made by probing a series of spots composing a line (40 μm with 9 spots) across the surface of ionocytes and adjacent keratinocytes (pavement cells). The calculation of NH_4^+ flux followed previous reports (Faszewski and Kunkel 2001; Donini and O’Donnell 2005).

Voltage gradients obtained from the ASET software were converted into concentration using the following equation:

$$\Delta C = C_b \times 10^{(\Delta V/S)} - C_b, \quad (2)$$

where ΔC is the concentration gradient between the two points measured in $\mu mol \cdot l^{-1} \cdot cm^{-3}$; C_b is the background ion concentration, calculated as the average of the concentration at each point measured in $\mu mol \cdot l^{-1}$; ΔV is the voltage gradient obtained from ASET in μV; and S is the slope of the electrode.

The concentration gradient was subsequently converted into flux using Fick’s law of diffusion in the following equation:

$$\boldsymbol{J} = \boldsymbol{D}(\Delta C) / \Delta x, \quad (3)$$

where $\boldsymbol{J}$ is the net flux of the ion in $pmol \cdot cm^{-2} \cdot s^{-1}$; $\boldsymbol{D}$ is the diffusion coefficient of the ion ($2.09 \times 10^{-5} \cdot cm^2 \cdot s^{-1}$ for NH_4^+ and $9.4 \times 10^{-5} \cdot cm^2 \cdot s^{-1}$ for H^+); ΔC is the concentration gradient in $pmol \cdot cm^{-3}$; and Δx is the distance between the two points measured in cm.

Concanavalin A (Con-A) labeling

Live larvae were incubated in normal water containing 0.5 mg/ml Alexa Fluor 488-conjugated Concanavalin (Con-A, Molecular Probes, Eugene, OR) for 10 min. After staining, the larvae were washed with normal water for 3 min.

Treatment with amiloride and bafilomycin A1

NHE nonspecific inhibitor amiloride was obtained from Sigma and used for investigating the role of NHE in NH_4^+ and H^+ excretion. Stock was prepared by dissolving amiloride into dimethyl sulfoxide (DMSO, Sigma). A final concentration of 100 μM was applied for blocking NHE function. A pre-test of amiloride affecting recording medium showed that the inhibitor had no influence on NH_4^+ and H^+ activity.

The specific H^+-pump inhibitor bafilomycin A1 (Sigma B-1793) was also used to examine the inhibitory effects on ammonium and proton secretion at the surface of larva skin. Bafilomycin A1 was dissolved in DMSO and added to the water media at final concentrations of 10 μM. Before measurement, larvae were pre-incubated in 10 μM bafilomycin A1 medium for 1 hour.

Morpholino designments and embryonic microinjection

To inhibit the expression of H^+-ATPase subunit A (*atp6v1a*) and Rhcg1(*drrhcg1*), morpholino oligonucleotide (MO) was obtained from Gene Tools (Philomath, OR), and injected into zebrafish larva. The MOs

against target genes were designed as follow:

atp6v1a: 5’-ATCCATCTTGTGTGTTAGAAAACTG-3’

drrhcg1: 5’-CAGTTGCCCATGTCTACAGCTTGAG-3’

A standard control MO(5’-CCTCTTACCTCAGTTACAATTTATA-3’) was used as the control. The standard control oligo provided by Gene Tools has no target and no significant biological activity. The MO solution was prepared with sterile water and contained 0.1% phenol red as a visualizing indicator. In the preliminary test and our previous study (Horng et al. 2007), embryos injected with 8 ng of control MO showed no significant difference in survival rate, morphology, or H^+ or NH_4^+ secretion (measured with SIET) compared with WT embryos, indicating that an injection of 8 ng control MO caused little or no specific effect. Therefore, 4-8 ng of H^+-ATPase or Rhcg1 MOs were microinjected into 1-4 cell stage embryo by IM-300 microinjector system (Narishigi Scientific Instrument Laboratory, Tokyo, Japan).

Reverse transcription-PCR

To extract mRNA for the initial step, appropriate amounts of adult zebrafish gill tissues were collected, homogenized in Trizol Reagent (Invitrogen, CA, USA), and treated for total RNA purification following the manufacturer’s protocol. To remove genomic DNA, extractant were treated with DNase I at 37℃ for 15 minutes. The amount and quality of total RNA were determined by measuring the absorbance at 260 nm and 280 nm with Nanodrop Spectrophotometer (PerkinElmer ND-1000, Delaware, USA). The completeness of total RNA was then checked by

RNA denatured gels. Total RNA from controlled and treated samples were diluted to equal concentration as template for reverse transcription (5 μg total RNA / reaction).

For cDNA synthesis, 5 μg of total mRNA were reverse-transcribed in a final volumn of 20 μl containing 0.5 mM dNTPs, 2.5 μM oligo (dT)18, 5 mM dithiothreitol and 200 units fo PowerScript reverse tanscriptase (Invitrogen) for 1.5 h at 42°C and followed by a 15-min incubation at 70 °C. For PCR amplification, 1 μl of cDNA was used as a template in a 25 μl final reaction volume containing 0.25 μM dNTP, 1.25 units of Gen-Taq polymerate (GeneMark, Taipei, Taiwan) and 0.2 μM of each primer.

Quantitative RT-PCR

To analysis the expression of target gene, quantitative RT-PCR (qRT-PCR) was applied. qRT-PCR was performed with an ABI7000 sequence detection system (ABI, Warrington, UK) in a final volume of 10 μl containing 5 μl of 2x SYBR green master mix (ABI), 50 nM of the primer pairs and 3.2 ng of cDNA. The standard curve of each gene was checked in a linear range with β-actin as an internal control. All the primer sets for qRT-PCR are shown in table 1.

Results

NH_4^+ secretion at the surface of zebrafish larvae

Surface NH_4^+ activity of 5-day post-fertilization (dpf) zebrafish larvae was measured with SIET to determine the NH_4^+ secretion by larval skin. Six spots on the surface of a larva were chosen for measurement: the snout (a), pericardial cavity (b), yolk-sac (c), trunk (d), cloaca (e), and tail (f) (Fig. 1A). $\Delta[NH_4^+]$ at the 6 spots was determined by calculating the difference between the target spot and background (~10 mm away from the larva). Figure 1B shows $\Delta[NH_4^+]$ values measured at the 6 spots from 4 individuals. $\Delta[NH_4^+]$ at the yolk sac was higher than at the other locations, indicating that NH_4^+ was mostly secreted in the yolk-sac area. When the microelectrode was moved step by step away from the yolk-sac surface, NH_4^+ activity gradually declined with distance (data not shown).

NH_4^+ flux in specific cell type of larval skin

Using NH_4^+ selective microelectrode, NH_4^+ flux at specific cells was measured by probing $\Delta[NH_4^+]$ at 10 μm intervals. Under microscope, ionocytes and keratinocytes (pavement cells) can be easily identified by their morphology (Fig. 2A). The measured ionocytes located mainly in the border between yolk-extension and trunk of the larvae. Figure 2B shows a serial probing (line scan) over the surface of an ionocyte which was further identified as HRC by fluorescent Con-A which is a specific and vital marker for HRC (Lin et al. 2006; Fig. 2C). The SIET detected weaker outward flow of NH_4^+ on keratinocytes but gradually increased

when probing toward the apical surface of the HRC (Fig. 2B). In contrast, no surge of signal was found when probing over the surface of Con-A negative cells (other type of ionocytes). Figure 2D shows the comparison of NH_4^+ flux (in pmole/cm^2. s) in HRC (Con-A$^+$, 5.84 ± 2.89, n=37), other ionocytes (Con-A$^-$, 2.34 ± 0.97, n=23), and pavement cell (PVC, 1.68 ± 1.56, n=50). The flux from HRC is about 3 folds higher than that from other cell types.

NH_4^+ secretion in larvae acclimated to high ammonium (HA)

Since the yolk-sac area contributes dominant NH_4^+ secretion in the larvae, this area was chosen for the measurement of NH_4^+ secretion. $\Delta[NH_4^+]$ was measured in the 5dpf larvae which had been pre-acclimated to various concentration of NH_4^+ (0, 0.5, 5, 10 mM) for 5 days (Fig. 3A). During the acclimation, no significant increase of mortality was found even in 10 mM HA, indicating that zebrafish can tolerant the HA. When measuring the larvae in the recording medium (contains 0.1 mM NH_4Cl), the NH_4^+ secretion shows a dose-dependent increase with the treated $[NH_4^+]$ (Fig. 3A; in mM: NW, 0.022 ± 0.004; HA(0.5), 0.037 ± 0.011; HA(1), 0.048 ± 0.012; HA(5), 0.073 ± 0.009; HA(10), 0.168 ± 0.035). Moreover, the NH_4^+ secretion of larvae also increased with development from 3 to 7 dpf (Fig. 3B). At 7dpf, $\Delta[NH_4^+]$ was measured at the surface of gills instead of yolk sac which was remarkably absorbed. In these stages, the NH_4^+ secretion was significantly higher in larvae exposed to 5 mM HA than larvae in NW (Fig. 3B).

H^+ secretion in larvae acclimated to HA

Surface H^+ gradient at yolk-sac area of the larvae was also measured with SIET to compare the effects of HA on larval acid secretion. The $\Delta[H^+]$ is positive and gradually increases with development in NW larvae (Fig. 4; in μM: 3dpf, 0.028 ± 0.009; 4dpf, 0.071 ± 0.013; 5dpf, 0.094 ± 0.019). However, the $\Delta[H^+]$ of HA larvae is significantly lower than that of NW larvae (in μM: 3dpf, 0.017 ± 0.005; 4dpf, 0.018 ± 0.014; 5dpf, 0.011 ± 0.005), particularly in larvae exposed to HA for 5 days (the 5 dpf larvae). At that time, the $\Delta[H^+]$ of HA decreased to about 10% of control.

Effects of external pH and strong buffer on ammonium secretion

The NH_4^+ gradient in NW larvae were measured in the recording media with different pH to examine the effect of external pH on ammonium secretion. Results show that the $\Delta[NH_4^+]$ is significantly higher in pH 6 medium than in pH 7 or pH 8 medium (Fig. 5A; in mM: pH 6, 0.076 ± 0.016; pH 7, 0.059 ± 0.014; pH 8, 0.048 ± 0.006; one-way ANOVA, Tukey's comparison, $p < 0.05$). When measuring the larvae in the medium with strong buffer (Fig. 5BC, 5 mM MOPS), both $\Delta[NH_4^+]$ and $\Delta[H^+]$ decrease to 64% (in mM: Control, 0.025 ± 0.004; MOPS, 0.016 ± 0.004) and 54% (in μM: Control, 0.063 ± 0.013; MOPS, 0.034 ± 0.01), respectively. These experiments indicate that the ammonium secretion from larval skin is closely linked to the surface pH.

Ammonium secretion in the larvae with gene knockdown or inhibitor treatment

To investigate the role of V-type H^+-ATPase in NH_4^+ secretion, morpholino gene knockdown (against *atp6v1a* gene) and bafilomycin A1 inhibition were conduced in this experiment. As shown in Fig. 6A, B, in the *atp6v1a* morphant (the larvae injected with morpholino oligonucleotides), both $\Delta[NH_4^+]$ (in mM: WT, 0.025 ± 0.005; Morphant, 0.009 ± 0.008) and $\Delta[H^+]$ (in μM: WT, 0.051 ± 0.013; Morphant, 0.016 ± 0.007) were decreased remarkably. The inhibited level of the ammonium and acid secretion are both close to 70%. This inhibitory effect is also confirmed by bafilomycin A1 treatment (10 μM for 1h) which significantly decrease both acid and ammonium secretion from larval skin (Fig. 7A; in mM: Control, 0.025 ± 0.004; Treated, 0.01 ± 0.007; Fig. 7B; in μM: Control, 0.060 ± 0.015; Treated, 0.015 ± 0.004). In the larvae injected with *drrhcg1* morpholino, the $\Delta[NH_4^+]$ decreased 36% (Fig. 6C; in mM: WT, 0.050 ± 0.008; Morphant, 0.032 ± 0.009), however, the $\Delta[H^+]$ was maintained at the same level (Fig. 6D; in μM: WT, 0.082 ± 0.017; Morphant, 0.073 ± 0.031). In addition, NH_4^+ fluxes were measured in HRCs of morphants or WT (Fig. 8). The NH_4^+ flux was significantly decreased in morphants (in pmole/cm^2. s: WT, 8.47 ± 3.38; Morphant, 3.99 ± 2.04).

To further examine if NHE also contributes to the ammonium secretion, amiloride (100 μM for 10 min) was applied to the larvae. Compare with bafilomycin, the inhibited level by amiloride (in mM: Control, 0.043 ± 0.006; Treated, 0.036 ± 0.007) is relatively low, and the

decreasing level of acid (in μM: Control, 0.115 ± 0.03; Treated, 0.092 ± 0.021) are similar to that by ammonium (Fig. 7C, D).

mRNA expression of *atp6v0c, znhe3b, drrhcg1* and *drrhcg2* in gills of adult zebrafish

mRNA expression of 4 genes, *atp6v0c* (H^+-ATPase), *znhe3b* (Na^+/H^+ exchanger), *drrhcg1* (Rhcg1) and *drrhcg2* (Rhcg2), were analyzed with qRT-PCR from gills of NW- or HA-zebrafish (acclimated to 5 mM NH_4Cl for 5 days). Only *drrhcg2* was significantly elevated by HA, the other 3 genes were not significantly changed (Fig. 9).

Discussion

In the present study, I examined the mechanism of ammonia transport in post-hatched zebrafish larvae. The major findings were: (1) ammonia is mainly excreted from the yolk-sac epithelium, in which HRCs secrete higher levels of acid and ammonia than do other epithelial cells; (2) the V-type H^+-pump in HRCs plays a critical role in ammonia transport by generating an external acid layer to drive transepithelial ammonia transport; and (3) Rhcg1 is involved in skin ammonia secretion.

In previous reports on fish ammonia transport, the net flux of total ammonia (including NH_3 and NH_4^+) was determined by calculating changes in total ammonia in the water during the experiment (Wright et al., 1993; Wilson et al., 1994). However, that method provides the ammonia flux from the entire animal but not specific organs or cell types. In this study, an ion-selective electrode technique (SIET) was used to measure the NH_4^+ activity and flux at specific locations on the surface of larval skin. The SIET has been used to detect various ions including H^+, K^+, Na^+, Ca^{2+}, Cl^-, etc. (Smith et al., 1994; Breton et al., 1996; Land et al., 1997; Shirihai et al., 1998; Smith and Trimarchi, 2001) of samples ranging from plants to animals. Unlike traditional ion-selective microelectrodes which are used to measure intra- or extracellular ion activities, the SIET detects extracellular ion activity and ion flux at specific locations. The application of SIET to probing NH_4^+ has been reported in studies of plant root absorption (Henriksen et al., 1990) and mosquito NH_4^+ excretion (Donini and O'Donnell, 2005). For the first

time, the present study used the SIET to detect cellular NH_4^+ transport in an intact vertebrate model, the zebrafish.

In this study, the ammonia secreted by larval skin was presented as $\Delta[NH_4^+]$ calculated from the difference in NH_4^+ activities between the background and the location of interest. To calibrate the NH_4^+ activity and flux, a linear Nernstean regression was done using a series of known concentrations of NH_4Cl. The slope of the concentrations above 0.1 mM was fitted to a linear Nernstean slope of 58, but gradually decayed at concentrations below 0.1 mM (data not shown). However, the NH_4^+ content in NW was lower than 0.01 mmol, and was thus beyond the linear range of the calibrating line. For a practical and precise calibration, the NH_4^+ concentration in the medium for SIET measurement was raised by adding 0.1 mM NH_4Cl.

In previous studies, the SIET was used to determine H^+ transport in the skin of zebrafish larvae and was shown to be a good approach for examining ion transport in a zebrafish model (Lin et al., 2006; Horng et al., 2007). The present study further used SIET to examine ammonia transport in zebrafish and provided direct evidences for the cellular location and molecular mechanism of ammonia transport in zebrafish larvae. In a study on the air-breathing mudskipper (*Periopthalmodon schlosseri*), mitochondria-rich cells (MRCs) were suggested to be the location of branchial ammonia transport (Wilson et al., 2000b). In zebrafish, vH-MRCs (which refer to HRCs in our study) were also suggested to be involved in ammonia transport based on evidence of Rhcg1 in the apical membrane (Nakada et al., 2007a). Furthermore, pavement cells were also suggested to be involved in ammonia transport

of zebrafish (Nakada et al., 2007a), pufferfish (Nakada et al., 2007b), and rainbow trout (Nawata et al., 2007). However, those studies provide only molecular evidence for the localization of the ammonia transporter, and functional evidence on these cells has not been reported. In this study, the SIET detected outward NH_4^+ fluxes of about 3-fold higher in HRCs than in adjacent pavement cells or other ionocytes. This finding is consistent to our previous finding that HRCs are acid-secreting cells (Lin et al., 2006) and consequently drive a significant amount of NH_3 transport by the mechanism of "acid-trapping". Although the NH_4^+ flux in HRCs is relatively high, pavement cells should greatly contribute to overall NH_4^+ transport due their large number and surface area.

The unstirred acid layer facilitating branchial ammonia transport (by the acid-trapping mechanism) has been proposed and may be the dominant mechanism for ammonia excretion in freshwater teleosts (Wilkie, 2002; Evans et al., 2005). This mechanism of skin ammonia transport was demonstrated in larval zebrafish by the present data. A high external pH (pH 8) and strong MOPS buffer (5 mM) diminished the formation of the surface acid layer (acid gradient) and consequently ammonia transport. In addition, the acid gradient at the skin surface was greatly diminished in larvae acclimated to 5 mM HA (Fig. 4). These data can be interpreted as increased NH_3 secretion from HA larvae combined (consumed) with the secreted H^+ at the skin surface thus generated a higher NH_4^+ gradient. If a larva secretes total ammonia in the form of NH_4^+, we would expect to see a slight increase in the surface acid gradient instead of a decrease. Our data apparently do not support this point.

More importantly, we suggest that H^+-ATPase in the apical membrane of HRCs contributes more than 70% to the skin acid secretion and accompanying ammonia transport. Both bafilomycin inhibition and *atp6v1a* gene knockdown directly demonstrated the contribution of H^+-ATPase to NH_4^+ secretion. In contrast, CO_2 diffusion and H^+ transport by NHE contributed relatively little to acid and ammonia secretion. In gills of the mudskipper (*P. schlosseri*), NHE was suggested to play a critical role in active ammonium transport (Na^+/NH_4^+ exchange; Randall et al., 1999); however, recent studies do not support this mechanism in freshwater fish (Nawata et al., 2007). Our data show that amiloride (100 μM is a NHE-specific dose) inhibited both H^+ and NH_4^+ secretion by ~20%, and the blocked NH_4^+ secretion was more likely due to a decrease in acid trapping than to Na^+/NH_4^+ exchange.

Rh glycoproteins (members of the Amt/MEP/Rh superfamily) are generally thought to function as NH_3/NH_4^+ transporters in a broad range of species (Winkler, 2006). Recent studies suggested that Amt/MEP/Rh proteins are more likely being channel proteins that deprotonate NH_4^+ and conduct NH_3 (Khademi et al., 2004; Javelle et al., 2008). Four isoforms of the Rh protein (Rhag, Rhbg, Rhcg1, and Rhcg2) have been identified in the gill epithelium of zebrafish (Nakada et al., 2007a). Among them, Rhcg1 expression has been located in the apical membrane of HRCs in the yolk sac and gills (Nakada et al., 2007a). In this study, we further conducted a loss-of-function study (*drrhcg1* gene knockdown) to demonstrate the function of Rhcg1 in ammonia transport. In Rhcg1 morphants, about a 40% decrease in ammonia secretion but no significant change in acid secretion was revealed (Fig. 6, 8). This suggests that other

Rh isoforms (such as Rhbg and Rhcg2) might also be involved in ammonia transport, and thus the effect of Rhcg1 knockdown alone was not as high as H^+-ATPase knockdown or bafilomycin treatment. Taking this evidence together, we suggest a model that H^+-ATPase in HRCs generates an extracellular H^+ gradient to drive facilitative NH_3 diffusion through Rhcg1 in HRCs and possibly through other Rh glycoproteins in pavement cells. An ongoing study investigates the function and regulation of other isoforms in zebrafish.

Interestingly, similar mechanism for ammonia transport was found in mammal urinary system (Weiner and Hamm, 2007). In the renal collecting duct, apical RhCG and basolateral RhBG in acid-secreting intercalated cells (renal MR cells) were suggested to conduct NH_3 into lumen by acid-trapping. Our system with zebrafish embryo and SIET might also serve as a good model for investigating human renal disease.

In this study, qRT-PCR was used to examine the mRNA expression of branchial *atp6v0c* (H^+-ATPase), *znhe3b* (Na^+/H^+ exchanger), *drrhcg1* (Rhcg1) and *drrhcg2* (Rhcg2) in zebrafish exposed to 5 mM HA for 5 days. Significant increase was found only in *drrhcg2*, but not in the 3 other genes. In rainbow trout, however, 1.5 mM HA was found to increase branchial Rhcg2 and H^+-ATPase mRNA expression after 12 and 48 h exposure (Nawata et al., 2007). The inconsistency might be due to difference in species or duration of HA exposure. Further experiment needs to be done in the future to investigate the regulation of those genes in response to HA.

References

Allert N, Koller H, Siebler M. 1998. Ammonia-induced depolarization of cultured rat cortical astrocytes. Brain Res **782**:261-270.

Avella M, Bornancin M. 1989. Anew analysis of ammonia and sodium transport through the gills of fresh water rainbow trout (*Salmo gairdneri*). J Exp Biol **142**:155-175.

Breton S, Smith PJ, Lui B, Brown D. 1996. Acidification of the male reproductive tract by a proton pumping (H^+)-ATPase. Nat Med **2**:470-472.

Cameron JN, Heisler N. 1983. Studies of ammonia in the trout: physiochemical parameters, acid-base behavior and respiratory clearance. J Exp Biol **105**:107-125.

Claiborne JB, Edwards SL, and Morrison-Shetlar AI. 2002. Acid-base regulation in fishes: cellular and molecular mechanisms. J Exp Zool **293**: 302-319.

Cooper AJ, Plum F. 1987. Biochemistry and physiology of brain ammonia. Physiol Rev **67**:440-519.

Donini A, O'Donnell MJ. 2005. Analysis of Na^+, Cl^-, K^+, H^+ and NH_4^+ concentration gradients adjacent to the surface of anal papillae of the mosquito *Aedes aegypti*: application of self-referencing ion-selective microelectrodes. J Exp Biol **208**:603-610.

Edwards SL, Tse CM, Toop T. 1999. Immunolocalisation of NHE3-like immunoreactivity in the gills of the rainbow trout (*Oncorhynchus mykiss*) and the blue-throated wrasse (*Pseudolabrus tetrious*). J

Anat **195**:465-469.

Evans DH, Cameron JN. 1986. Gill ammonia transport. J Exp Zool **239**:17-23.

Evans DH, Piermarini PM, Choe KP. 2005. The multifunctional fish gill: dominant site of gas exchange, osmoregulation, acid-base regulation, and excretion of nitrogenous waste. Physiol Rev **85**:97-177.

Faszewski EE, Kunkel JG. 2001. Covariance of ion flux measurements allows new interpretation of Xenopus laevis oocyte physiology. J Exp Zool **290**:652-661.

Felipo V, Butterworth RF. 2002. Neurobiology of ammonia. Prog Neurobiol **67**:259-279.

Henriksen GH, Bloom AJ, Spanswick RM. 1990. Measurement of Net Fluxes of Ammonium and Nitrate at the Surface of Barley Roots Using Ion-Selective Microelectrodes. Plant Physiol **93**:271-280.

Hirata T, Kaneko T, Ono T, Nakazato T, Furukawa N, Hasegawa S, Wakabayashi S, Shigekawa M, Chang MH, Romero MF, Hirose S. 2003. Mechanism of acid adaptation of a fish living in a pH 3.5 lake. Am J Physiol Regul Integr Comp Physiol **284**:R1199-1212.

Horng JL, Lin LY, Huang CJ, Katoh F, Kaneko T, Hwang PP. 2007. Knockdown of V-ATPase subunit A (atp6v1a) impairs acid secretion and ion balance in zebrafish (*Danio rerio*). Am J Physiol Regul Integr Comp Physiol **292**:R2068-2076.

Huang CH, Liu PZ. 2001. New insights into the Rh superfamily of genes and proteins in erythroid cells and nonerythroid tissues. Blood Cells Mol Dis **27**:90-101.

Hung CY, Tsui KN, Wilson JM, Nawata CM, Wood CM, Wright PA. 2007. Rhesus glycoprotein gene expression in the mangrove killifish *Kryptolebias marmoratus* exposed to elevated environmental ammonia levels and air. J Exp Biol **210**:2419-2429.

Hwang PP, Lee TH. 2007. New insights into fish ion regulation and mitochondrion-rich cells. Comp Biochem Physiol A Mol Integr Physiol **148**:479-497.

Javelle A, Lupo D, Ripoche P, Fulford T, Merrick M, Winkler FK. 2008. Substrate binding, deprotonation, and selectivity at the periplasmic entrance of the *Escherichia coli* ammonia channel AmtB. Proc Natl Acad Sci U S A **105**:5040-5045.

Karnaky KJ, Jr., Kinter LB, Kinter WB, Stirling CE. 1976. Teleost chloride cell. II. Autoradiographic localization of gill Na,K-ATPase in killifish *Fundulus heteroclitus* adapted to low and high salinity environments. J Cell Biol **70**:157-177.

Land SC, Sanger RH, Smith PJ. 1997. O_2 availability modulates transmembrane Ca_2^+ flux via second-messenger pathways in anoxia-tolerant hepatocytes. J Appl Physiol **82**:776-783.

Lin LY, Horng JL, Kunkel JG, Hwang PP. 2006. Proton pump-rich cell secretes acid in skin of zebrafish larvae. Am J Physiol Cell Physiol **290**:C371-378.

Marini AM, Soussi-Boudekou S, Vissers S, Andre B. 1997. A family of ammonium transporters in Saccharomyces cerevisiae. Mol Cell Biol **17**:4282-4293.

Marshall WS, Lynch EM, Cozzi RR. 2002. Redistribution of immunofluorescence of CFTR anion channel and NKCC

cotransporter in chloride cells during adaptation of the killifish *Fundulus heteroclitus* to sea water. J Exp Biol **205**:1265-1273.

McDonald DG, Prior ET. 1988. Branchial mechanisms of ion and acid-base regulation in the fresh water rainbow trout, *Salmo gairdneri*. Can J Zool **66**:2699-2708.

McDonald DG, Wood CM. 1981. Branchial and renal acid and ion fluxes in the rainbow trout, *Salmo gairdneri*, at low environmental pH. J Exp Biol **93**:101-118.

Nakada T, Hoshijima K, Esaki M, Nagayoshi S, Kawakami K, Hirose S. 2007a. Localization of ammonia transporter Rhcg1 in mitochondrion-rich cells of yolk sac, gill, and kidney of zebrafish and its ionic strength-dependent expression. Am J Physiol Regul Integr Comp Physiol **293**:R1743-1753.

Nakada T, Westhoff CM, Kato A, Hirose S. 2007b. Ammonia secretion from fish gill depends on a set of Rh glycoproteins. FASEB J **21**:1067-1074.

Nawata CM, Hung CC, Tsui TK, Wilson JM, Wright PA, Wood CM. 2007. Ammonia excretion in rainbow trout (*Oncorhynchus mykiss*): evidence for Rh glycoprotein and H^+-ATPase involvement. Physiol Genomics **31**:463-474.

Ninnemann O, Jauniaux JC, Frommer WB. 1994. Identification of a high affinity NH_4^+ transporter from plants. EMBO J 13:3464-3471.

Randall DJ, Wilson JM, Peng KW, Kok TW, Kuah SS, Chew SF, Lam TJ, Ip YK. 1999. The mudskipper, *Periophthalmodon schlosseri*, actively transports NH_4^+ against a concentration gradient. Am J Physiol **277**:R1562-1567.

Salama A, Morgan IJ, Wood CM. 1999. The linkage between Na^+ uptake and ammonia excretion in rainbow trout: kinetic analysis, the effects of $(NH_4)_2SO_4$ and NH_4HCO_3 infusion and the influence of gill boundary layer pH. J Exp Biol **202**:697-709.

Shirihai O, Smith P, Hammar K, Dagan D. 1998. Microglia generate external proton and potassium ion gradients utilizing a member of the H^+/K^+ ATPase family. Glia **23**:339-348.

Smith PJ, Sanger RH, Jaffe LF. 1994. The vibrating Ca^{2+} electrode: a new technique for detecting plasma membrane regions of Ca^{2+} influx and efflux. Methods Cell Biol **40**:115-134.

Smith PJ, Trimarchi J. 2001. Noninvasive measurement of hydrogen and potassium ion flux from single cells and epithelial structures. Am J Physiol Cell Physiol **280**:C1-11.

Walsh PJ. 1998. Nitrogen excretion and metabolism. In: Evans DH, editor. The physiology of fishes. Boca Raton: CRC Press. p 199-214.

Weiner ID. 2006. Expression of the non-erythroid Rh glycoproteins in mammalian tissues. Transfus Clin Biol **13**:159-163.

Weiner ID, Hamm LL. 2007. Molecular mechanisms of renal ammonia transport. Annu Rev Physiol **69**:317-340.

Westhoff CM, Siegel DL, Burd CG, Foskett JK. 2004. Mechanism of genetic complementation of ammonium transport in yeast by human erythrocyte Rh-associated glycoprotein. J Biol Chem **279**:17443-17448.

Wilkie MP. 2002. Ammonia excretion and urea handling by fish gills: present understanding and future research challenges. J Exp Zool

293:284-301.

Wilson JM, Laurent P, Tufts BL, Benos DJ, Donowitz M, Vogl AW, Randall DJ. 2000a. NaCl uptake by the branchial epithelium in freshwater teleost fish: an immunological approach to ion-transport protein localization. J Exp Biol **203**:2279-2296.

Wilson JM, Randall DJ, Donowitz M, Vogl AW, Ip AK. 2000b. Immunolocalization of ion-transport proteins to branchial epithelium mitochondria-rich cells in the mudskipper (*Periophthalmodon schlosseri*). J Exp Biol **203**:2297-2310.

Wilson RW, Wright PM, Munger RS, Wood CM. 1994. Ammonia excretion in fresh water rainbow trout (*Oncorhynchus mykiss*) and the importance of gill boundary layer acidification: lack of evidence for Na^+/NH_4^+ exchange. J Exp Biol **191**:37-58.

Winkler FK. 2006. Amt/MEP/Rh proteins conduct ammonia. Pflugers Arch **451**:701-707.

Wood CM. 1993. Ammonia and urea metaboism and excretion. In: Evans DH, editor. The Physiology of Fishes. Boca Raton: CRC Press. p 379-425.

Wright PA. 1993. Nitrogen excretion and enzyme pathways for ureagenesis in fresh water tilapia (*Oreochromis niloticus*). Physiol Zool **66**:881-901.

Wright PA, Randall DJ, Perry SF. 1989. Fish gill boundary layer: a site of linkage between carbon dioxide and ammonia excretion. J Comp Physiol **158**:627-635.

Yan JJ, Chou MY, Kaneko T, Hwang PP. 2007. Gene expression of Na^+/H^+ exchanger in zebrafish H^+-ATPase-rich cells during acclimation

to low-Na^+ and acidic environments. Am J Physiol Cell Physiol **293**:C1814-1823.

Table 1. Primer sets for quantitative RT-PCR

Gene	Primer Sequence
atp6v0c	
	F 5’ GAGGAACCACTGCCATTCCA 3’
	R 5’ CAACCCACATAAATGATGACATCG 3’
nhe3b	
	F 5’ TGCAGACAGCGCCTCTAGC 3’
	R 5’ TGTGGCCTGTCTCTGTTTGC 3’
drrhcg1	
	F 5’ TGCCAACTGTCCAGGGTG 3’
	R 5’ AGGATAAGACGGGAGGAATAAT 3’
drrhcg2	
	F 5’ CTTTGGTTGGTGGCATACTAA 3’
	R 5’ GCATCTGGCGTCCTTTCT 3’
β-actin	
	F 5’ ATTGCTGACAGGATGCAGAAG 3’
	R 5’ GATGGTCCAGACTCATCGTACTC 3’

F: Forward primer
R: Reverse primer

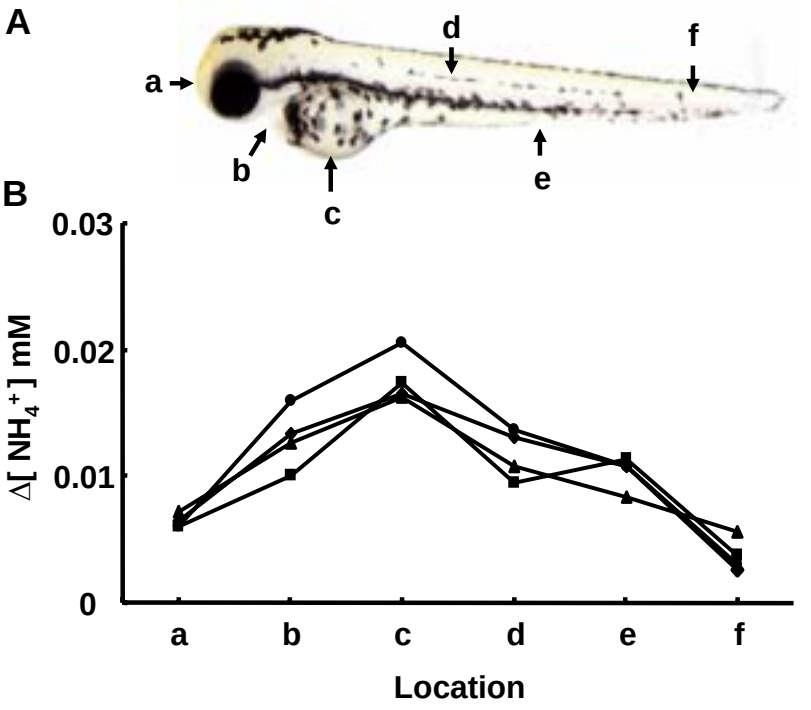

Fig. 1. Ammonium gradient ($\Delta[NH_4^+]$) at the surface of a zebrafish larva. (A) Shows the 6 spots measured with ion-selective electrode technique (SIET): (a) snout, (b) pericardial cavity, (c) yolk-sac, (d) trunk, (e) cloaca, and (f) tail. (B) Shows the $\Delta[NH_4^+]$ measured at 6 spots of 4 individuals.

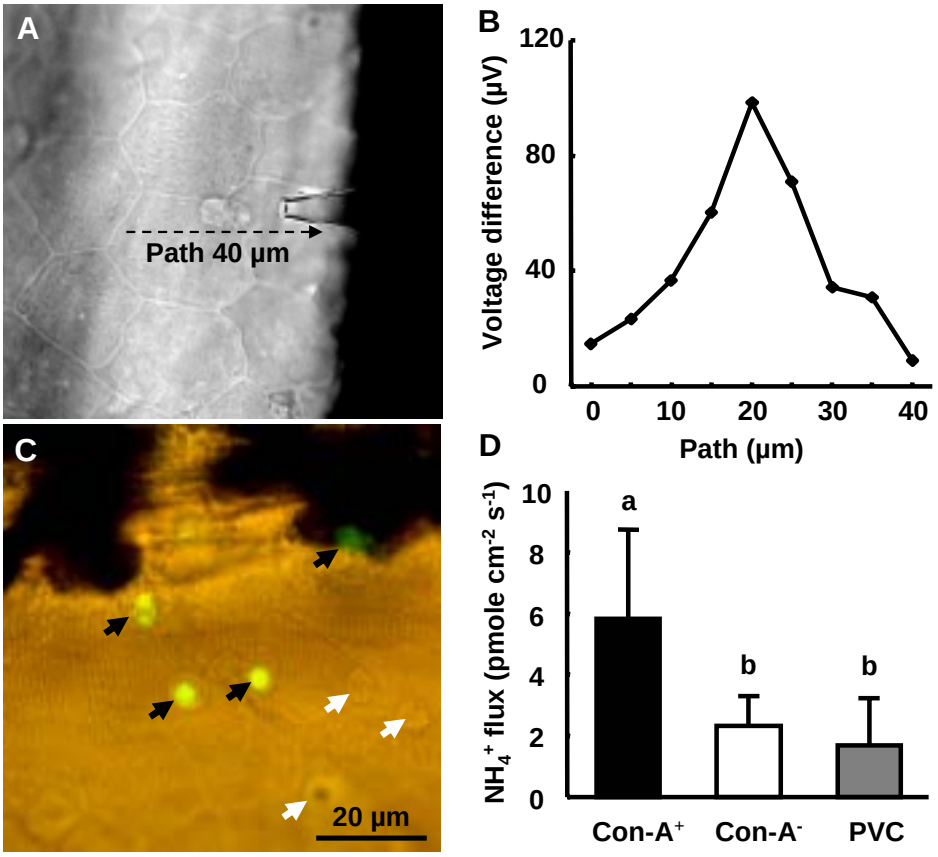

Fig. 2. NH_4^+ fluxes at H^+ pump-rich cells (HRCs) (Con-A^+), keratinocytes (pavement cells, PVCs), and other ionocytes (Con-A^-). Under a microscope, apical membranes of ionocytes were identified, and a "line scan" was made by probing at a series of locations along a line (arrow) across the surface of the ionocytes and adjacent keratinocytes (A). (B) Shows the measured NH_4^+ fluxes of the line scan over the surface of an HRC. The measured ionocytes were further discriminated into a Con-A^+ (HRC) or Con-A^- (non-HRC) group by fluorescent Con-A labeling (C). NH_4^+ effluxes (mean ± SD, n = 37, 23, 50 respectively) from different types of cells were compared (D). Different letters indicate a significant difference (one-way ANOVA, $p < 0.05$).

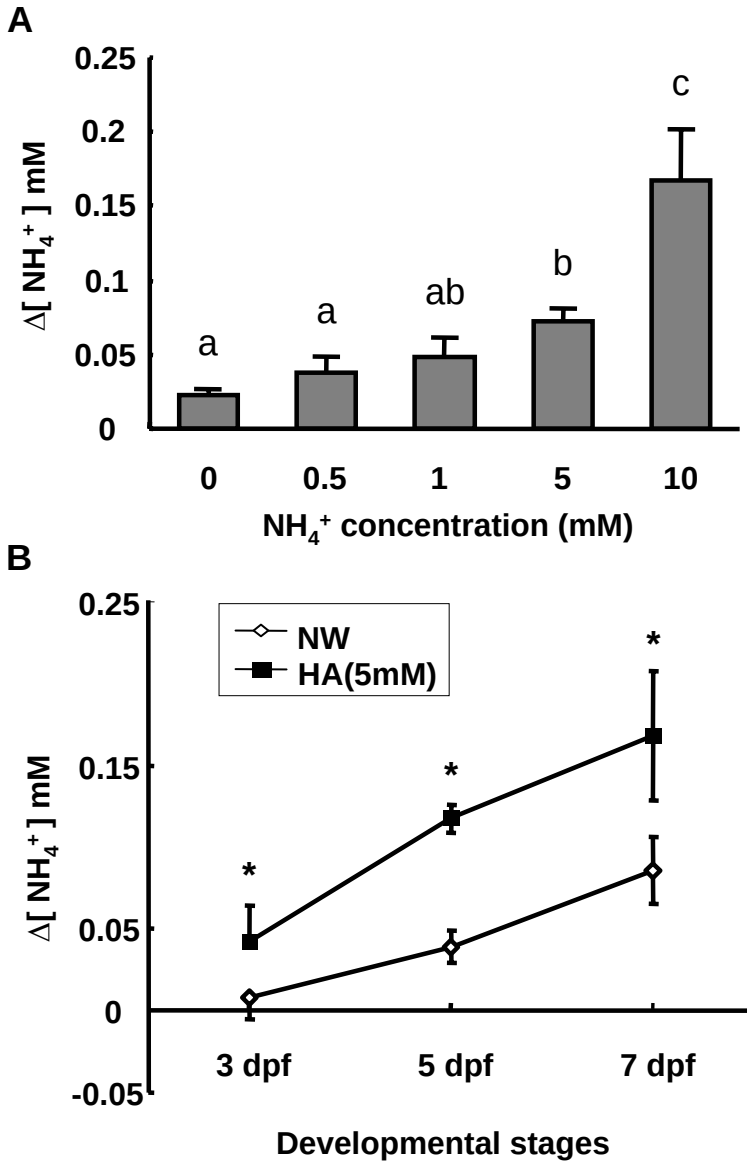

Fig. 3. (A) Ammonia gradient ($\Delta[NH_4^+]$) at the yolk sac surface of larvae acclimated to various concentrations (0~10 mM) of NH_4Cl (one-way ANOVA, Tukey's comparison, $p < 0.05$). (B) Developmental change in $\Delta[NH_4^+]$ at the yolk sac surface of larvae acclimated to normal water (NW) or high ammonium (HA; 5 mM). In 7 days post-fertilization (dpf) larvae, gills were measured because of the disappearance of the yolk sac. Data are presented as the mean ± SD ($n = 10$). * Indicates a significant difference between NW and HA larvae at the same stage (Student's *t*-test, $p < 0.05$).

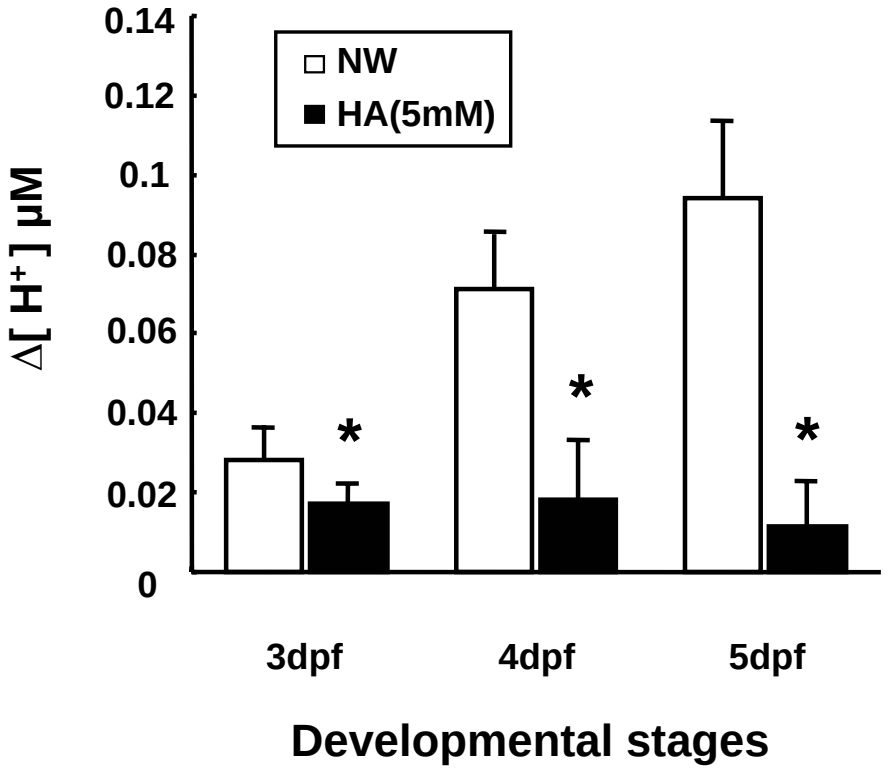

Fig. 4. H^+ gradient ($\Delta[H^+]$) at the yolk-sac surface of larvae acclimated to normal water (NW) or high ammonia (HA; 5 mM). Three developmental stages (3, 4, and 5 days post-fertilization; dpf) are shown. Data are presented as the mean ± SD (n = 10). * Indicates a significant difference between NW and HA larvae at the same stage (Student's t-test, $p < 0.05$).

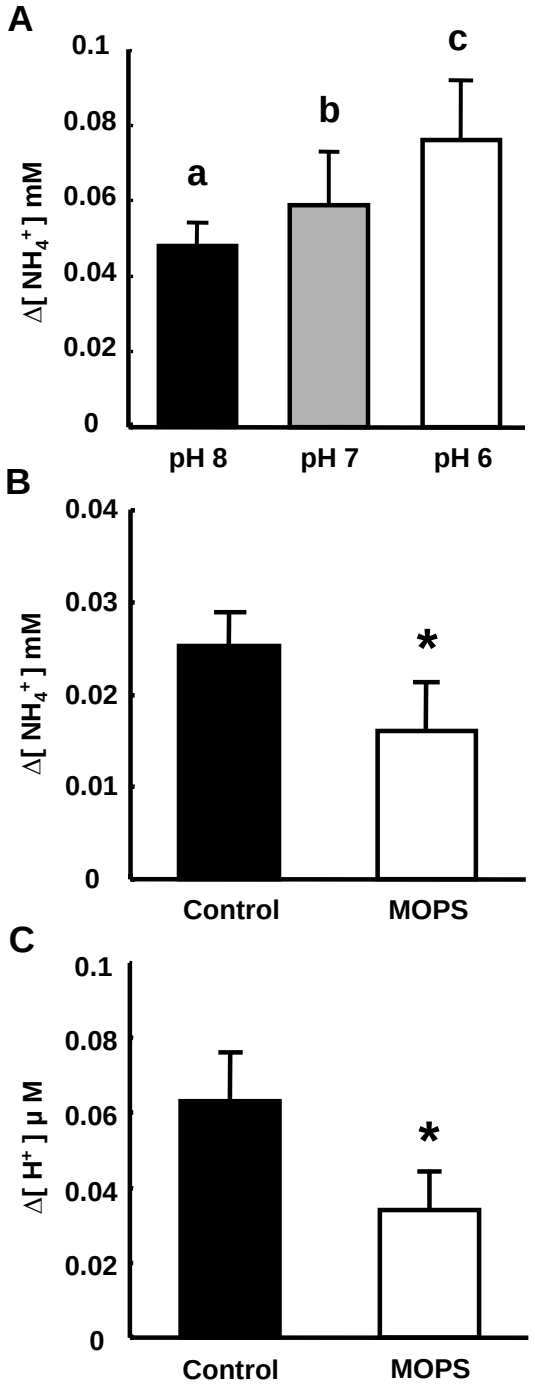

Fig. 5. Effects of external pH (A) and MOPS buffer (5 mM) on the ammonia gradient ($\Delta[NH_4^+]$) (B) and H+ gradient ($\Delta[H^+]$) (C) at the yolk-sac surface of larvae. Data are presented as the mean ± SD (n = 10). Different letters indicate a significant difference between pH 6, pH 7, and pH 8 (one-way ANOVA, Tukey's comparison, $p < 0.05$). * Indicates a significant difference between the normal water (NW) and MOPS groups (Student's t-test, $p < 0.05$).

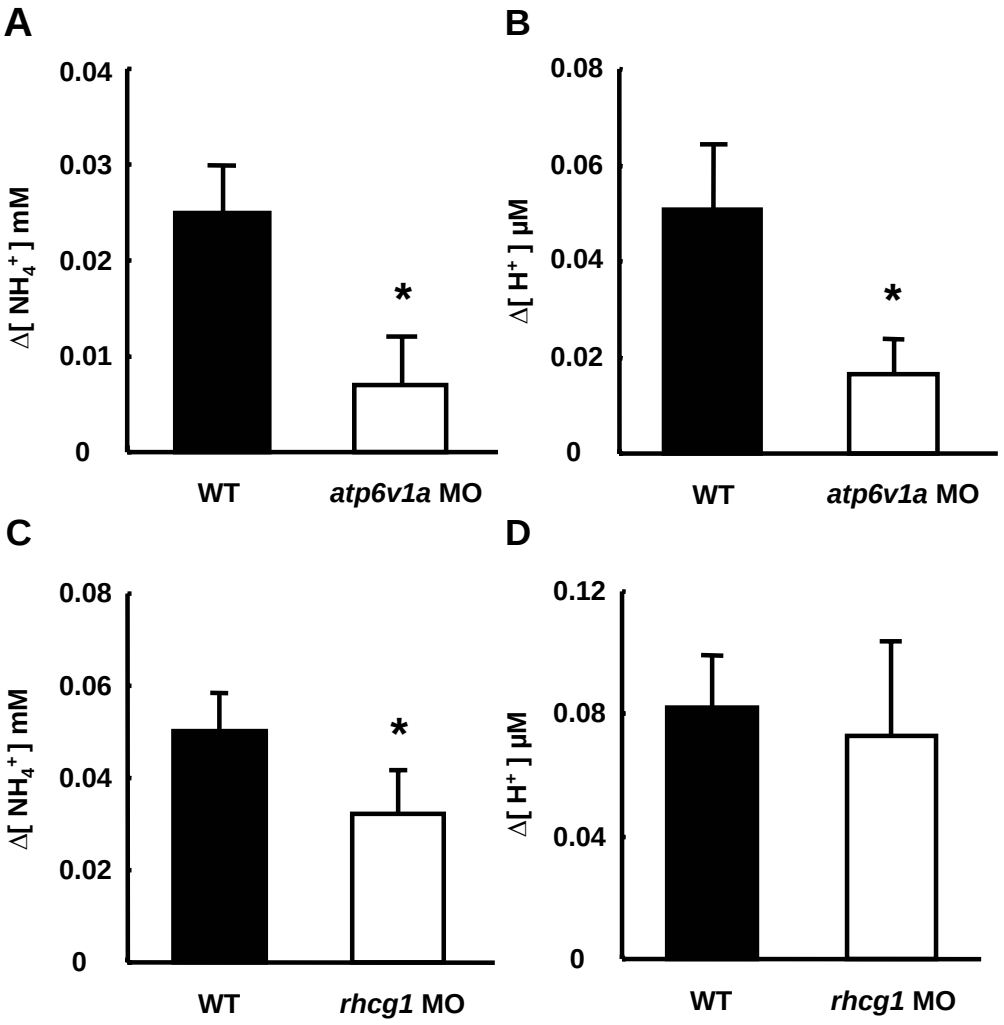

Fig. 6. Ammonia gradient ($\Delta[NH_4^+]$) (A, C) and H^+ gradient ($\Delta[H^+]$) (B, D) at the yolk-sac surface of wild-type (WT) larvae and morpholino (MO)-injected larvae. The morpholino against *atp6v1* or *rhcg1* was injected at the 1~4-cell stage of larvae, and the larvae were measured at 5 days post-fertilization (dpf). Different batches of embryos were used for the *atp6v* or *rhcg1* injection. Data are presented as the mean ± SD (n = 10). * Indicates a significant difference (Student's t-test, $p < 0.05$).

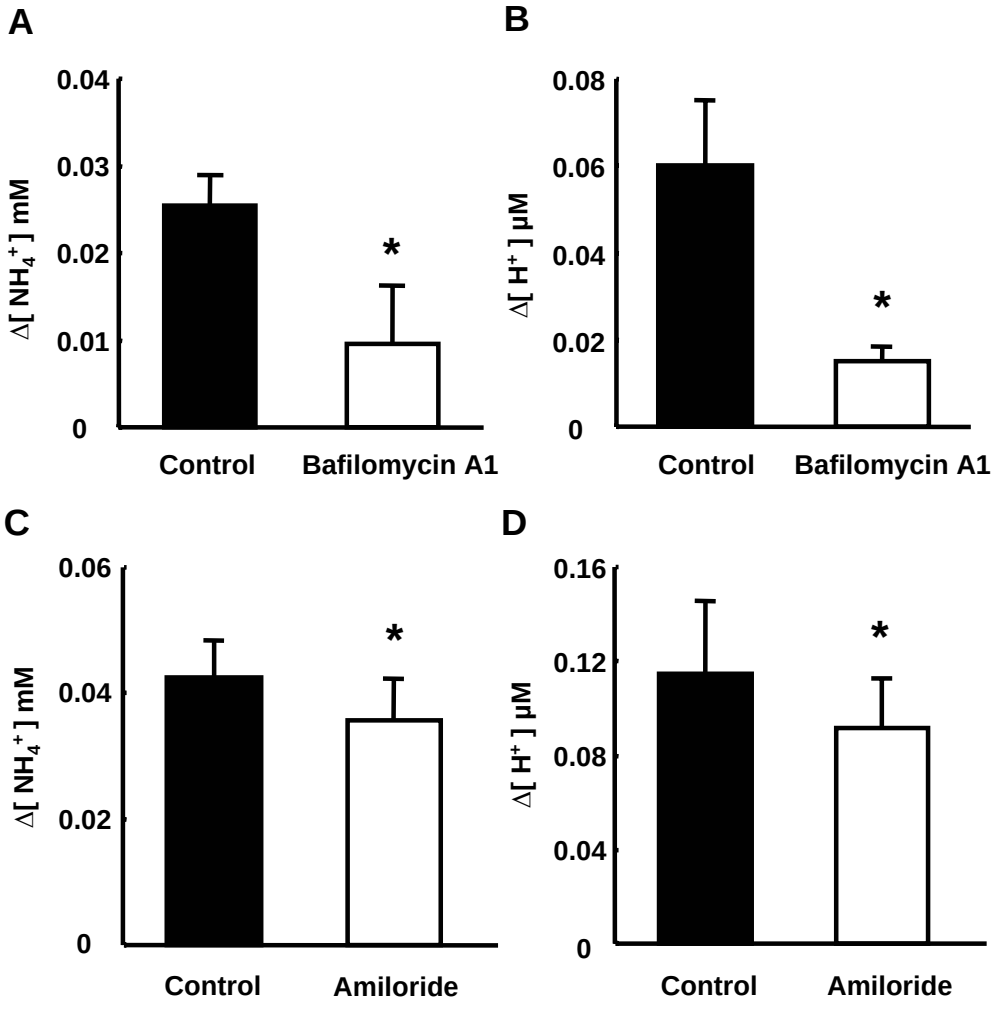

Fig. 7. Effects of bafilomycin A1 and amiloride on the ammonia gradient ($\Delta[NH_4^+]$) (A, C) and H^+ gradient ($\Delta[H^+]$) (B, D) at the yolk-sac surface of zebrafish larvae. Different batches of 5-day post-fertilization (dpf) larvae were used for bafilomycin A1or amiloride treatments. Data are presented as the mean ± SD (n = 10). * Indicates a significant difference (Student's t-test, $p < 0.05$).

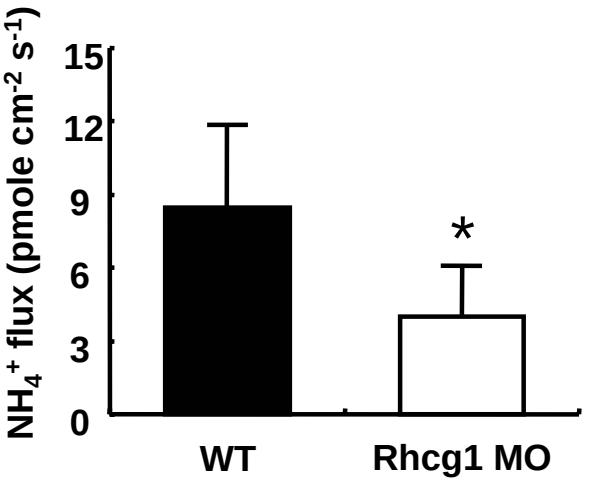

Fig.8 . NH_4^+ flux in the HRC of WT and Rhcg1 MO fishes. 4-dpf* fish larva were selected for cell flux measurement. * indicate significant difference between WT (n = 10) and Morphant (*n* = 10) (Student's *t*-test, $p < 0.05$).

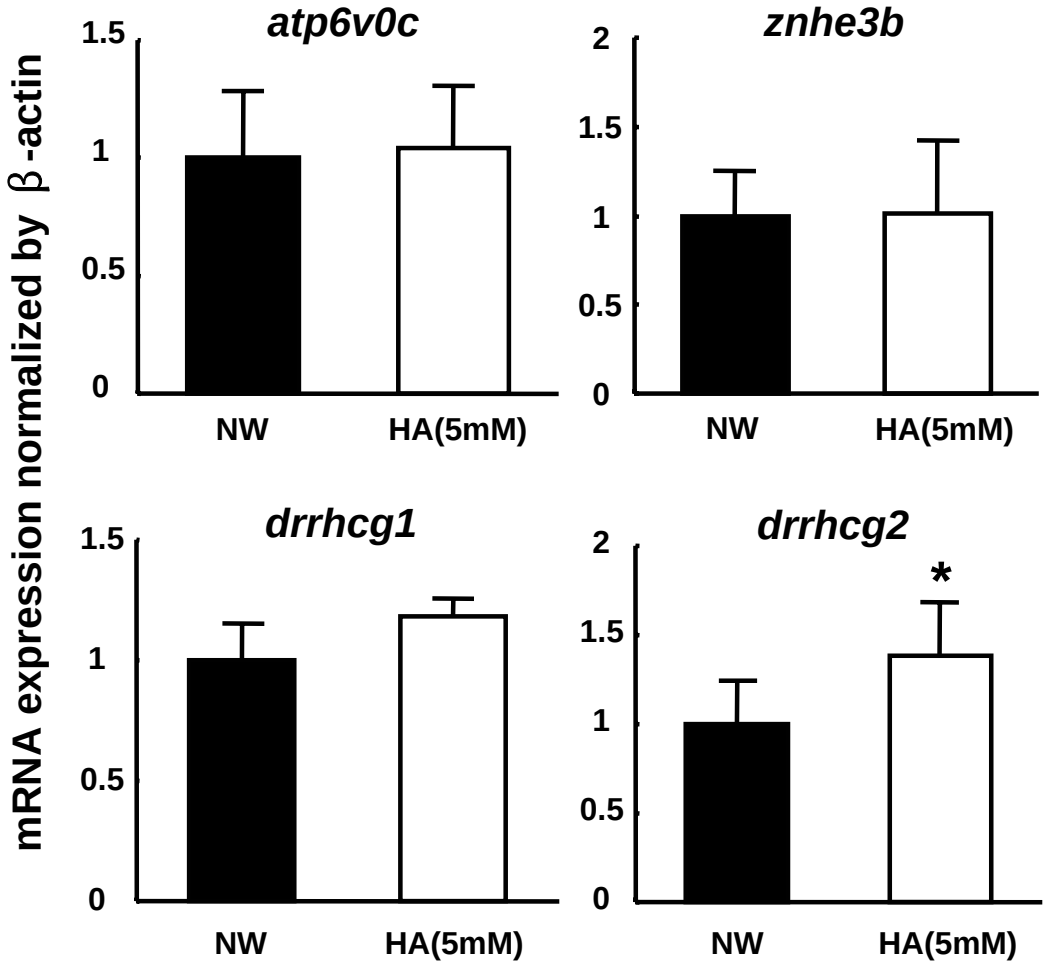

Fig. 9. Transcripts of *atp6v0c*, *znhe3b*, *zfrhcg1* and *zfrhcg2* in gills of NW and HA(5mM) zebrafish. Analysis the mRNA expression of H+-pump subunits ATP6v0c(A), zebrafish Na^+/H^+ exchanger zNHE3b (B), zebrafish Rhesus glycoprotein zfRhcg1 (C) and zfRhcg2 (D) were performed by qRT-PCR. mRNA expression levels were normalized by β–actin. Only zfRhcg1 mRNA were upregulated after 5days [NH_4^+] 5mM treatment. * indicate significant difference between NW and HA(5mM) fishes (Student's *t*-test, $p < 0.05$).